Numerical study of turbulent flow and thermal field in industrial electrotechnological devices with combined power supply

S Pavlovs, A Jakovics, V Sushkovs, B Nacke

Numerical study of turbulent flow and thermal field in industrial electrotechnological devices with combined power supply

S. Pavlovs[1], A. Jakovics[1], V. Sushkovs[1], B. Nacke[2]

[1]Laboratory for Mathematical Modelling of Environmental and Technological Processes,
University of Latvia, 8 Zellu str., LV-1002, Riga, Latvia
[2]Institute of Electrotechnology, Leibniz University of Hannover,
Wilhelm-Busch-Str. 4, D-30167 Hannover, Germany

Corresponding author: sergejs.pavlovs@lu.lv

Abstract
The paper presents the numerical 3D models for computations of turbulent hydrodynamic and thermal fields for the electrotechnological devices with the combined power supply: conductive – over the submerged or non-submerged electrodes with direct current (DC); inductive – with the side inductor, the source of travelling magnetic field (TMF).
The thermal field distribution and the overheating zones are considered for conditions, when the heat flux is supplied to the melt over the arc spot, which located under non-submerged or submerged tip of the top electrode. The structure and intensity of the melt circulation is discussed for the cases of high and low conductivity of melt.

Key words: combined inductive and conductive power supply, turbulent flow, thermal field, LES study

Introduction

The current paper is a continuation of numerical study of the 3D physical fields in the electrotechnological magnetohydrodynamic (MHD) devices with the combined power supply: inductive by the inductor and conductive through the electrodes; the main results are presented in [1,2]. Some examples of the MHD devices are electrical arc furnaces (EAF), ladle furnaces (LF), plasma furnaces (PF), etc. The purpose of research is the application of developed 3D models for analysis of various technological regimes in order to obtain a desired quality of melts and alloys.
The melt circulation [1] is a result of the combination of electro-vortex convection (EVC) and electromagnetic convection (EMC). The cross effects of the interaction between the current and a magnetic field produced by different alternating current (AC) sources affect mainly the pattern and intensity of the resultant flow and may cause rotation.
The temperature field [2] in a turbulently flowing melt is modelled according to the thermal balance of heat exchange at the melt boundaries and the Joule heat volumetric sources produced by different types of AC power supply.
The current paper is concerned with the numerical computations of a temperature field and a melt circulation in MHD devices with combined power supply (Fig. 1), which widen the application of the developed 3D models:
• conductive – DC is supplied through the top (non-submerged or submerged) and the bottom electrodes
• inductive – AC is supplied by the side inductor, the source of upwards travelling magnetic field.

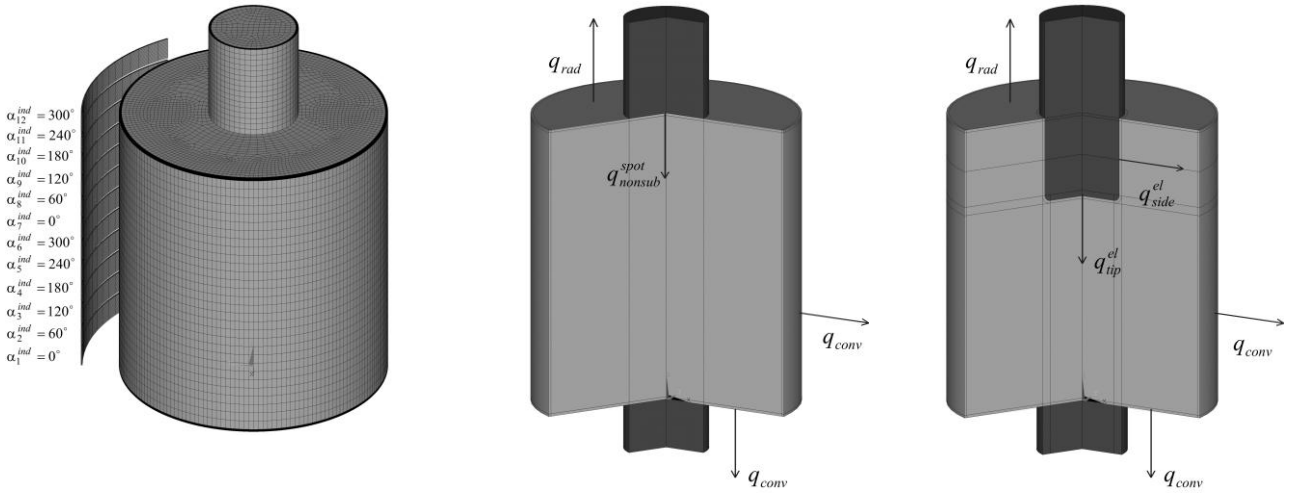

(a) (b) (c)

Fig. 1: 3D models of MHD device with top and bottom DC electrodes and side inductor, the source of upwards TMF: (a) structured mesh; AC phases in inductor; (b,c) thermal fluxes for non-submerged and submerged electrode.

Peculiarities of electromagnetic (EM) field computations

In the case of combined power supply the numerical solutions of the Maxwell equations must be found separately for the conductively supplied DC (over electrodes) and the inductively supplied AC (with inductor). The computations have been performed with ANSYS Multiphysics 14.0 using a static and a harmonic analysis accordingly. For approximation of the model geometry (Fig. 1) the element SOLID97 is used. The equations (real and complex accordingly) are solved with the direct method. The total number of equations is ~1.8 million.

The density of time-averaged total Lorentz force $\vec{\bar{f}}^{\,EM}$ is found according to the superposition principle:

$$\vec{\bar{f}}^{\,EM} = \vec{j}_{DC}^{\,cond} \times \vec{B}_{DC}^{\,cond} + \frac{1}{2}\Re e\left(\underline{\vec{j}_{AC}^{\,ind}} \times \underline{\vec{B}_{AC}^{\,*ind}}\right) \qquad (1)$$

where $\vec{j}_{DC}^{\,cond}$ is a current density, supplied over the electrodes, and $\vec{B}_{DC}^{\,cond}$ is an induction of self magnetic field of the conductive DC (indexes 'cond' and 'DC'); $\underline{\vec{j}_{AC}^{\,ind}}$ is an amplitude value of a current density and $\underline{\vec{B}_{AC}^{\,*ind}}$ is a conjugate value of magnetic induction in case of the complex representation of quasi-stationary EM field, produced by the inductor with AC (indexes 'ind' and 'AC').

The density of total Joule heat Q^{EM} is the sum of Joule heat due to conductive Q_{melt}^{cond} and inductive Q_{melt}^{ind} power supply. The distributions of the total Lorentz force components and the total Joule heat are computed by means of the summation of corresponding distributions, obtained during the EM field computations, performed for both types of power supply. As these two sets of the results are obtained at the different meshes, the summation operation of Lorentz force and Joule heat for the different sources is performed in ANSYS CFX 14.0 with application of the build-in tools of interpolation to the mesh, which is used for the computations of HD and thermal fields.

The mentioned above approach differs from referenced computations, which have been performed only for a single source of power, supplied over the DC electrodes; examples are chosen for several types of industrial equipment and processes – EAF [3,4], vacuum arc (VAR) [5] or electro-slag remelting (ESR) [6], submerged arc furnaces (SAF) [7].

Peculiarities of thermal field computations

The thermal field modelling is performed only for the melt (Fig. 1 (b,c)) with ***the following assumptions*** concerned with melt heating during conductive power supply through the top electrode:

• in the case of the non-submerged top electrode: an electric arc is burned between the electrode and the arc spot zone at the melt top surface;

• in the case of the submerged top electrode: an electric arc is burned between the tip of electrode and melt;

• the area of the spot (for non-submerged electrode) or the area of the tip (for submerged electrode) are equal to the area of the electrode horizontal cross-section;

• the heat flux from the electrical arc is supplied to the melt over the spot (for non-submerged electrode) or over the tip of electrode (for submerged electrode).

The thermal boundary conditions are determined for the following surfaces of the melt (Fig. 1 (b,c)):

• for the top surface radiative zone with the surface S_{rad} the radiation heat flux q_{rad} is determined;

• for the thermally insulated side and bottom solid wall with the surface S_{solid} of the melt vessel the convective heat exchange flux q_{conv} is determined;

• in the case of the non-submerged electrode: for the surface S^{spot} the heat flux q_{nonsub}^{spot} from the arc directed to the melt is determined:

$$\lambda_{melt}\left.\frac{\partial T}{\partial n}\right|_{S^{spot}} = -q_{nonsub}^{spot} \qquad q_{nonsub}^{spot} = \frac{q_{rad}\cdot S_{rad} + q_{conv}\cdot S_{solid} - \left(Q_{melt}^{ind} + Q_{melt}^{cond}\right)}{S^{spot}} \qquad (2)$$

where the value of heat flux q_{nonsub}^{spot} is found from the initial thermal balance.

• in the case of submerged electrode: for the surface S_{tip}^{el} the heat flux q_{tip}^{el} from the arc directed to the melt is determined as well as for the side surface S_{side}^{el} of the heated electrode the heat flux q_{side}^{el} is determined:

$$\lambda_{melt}\left.\frac{\partial T}{\partial n}\right|_{S_{tip}^{el}} = -q_{tip}^{el} \qquad \lambda_{melt}\left.\frac{\partial T}{\partial n}\right|_{S_{side}^{el}} = -q_{side}^{el}$$

$$q_{sub}^{el} = \frac{q_{rad}\cdot S_{rad} + q_{conv}\cdot S_{solid} - \left(Q_{melt}^{ind} + Q_{melt}^{cond}\right)}{a_{tip}S_{tip}^{el} + a_{side}S_{side}^{el}} \qquad q_{tip}^{el} = a_{tip}\,q_{sub}^{el} \qquad q_{side}^{el} = \left(1 - a_{tip}\right)q_{sub}^{el} \qquad (3)$$

where the value of the total heat flux q_{sub}^{el} from the electrode is found from the initial thermal balance. The total surface

of the electrode is $S_{sub}^{el} = S_{tip}^{el} + S_{side}^{el}$. The part a_{tip} (is the empirical coefficient) of the total heat flux q_{sub}^{el} is prevailing ~90–95% and the part is $a_{side} = 1 - a_{tip}$ ~5–10%.

The thermal parameters, which are used in boundary conditions (in details are written in [2]), are the following:

• the initial T_{init} =1820 K, cover T_{cov} =873 K and ambient T_a =330 K temperature values are identical for all models;

• the areas: S^{spot} ~0.58 m^2 (non-submerged electrode); S_{tip}^{el} ~0.64 m^2, S_{side}^{el} ~2.23 m^2 (submerged electrode); S_{rad} ~5.2 m^2.

• the heat transfer coefficient at the vessel surfaces with the thermal insulation, α_{solid} ~ 1.19 $W/(m^2 \cdot K)$.

Computational results

Maximum T_{max}, minimum T_{min} and overheating $\theta = T_{max} - T_{min}$ temperature values are compared for chosen models.

The relation of intensities for various types of the melt convection may be estimated with Alfven numbers Al_{cond} (for EVC) and Al_{ind} (for EMC) as well as with Froude number for Archimedes force Fr_A (for TGC – thermogravitational convection). The non-dimensional parameters may be found from the following expressions

$$Al_{cond} = \frac{j_{0,cond}^2 \mu_0 r_{melt}^2}{\rho v_{melt}^2} \qquad Al_{ind} = \frac{j_{0,ind}^2 \mu_0 r_{melt}^2}{\rho v_{melt}^2} \qquad Fr_A^{-1} = \frac{g \beta \theta r_{melt}}{v_{melt}^2} \tag{4}$$

where β, ρ, r_{melt} and v_{melt} are thermal expansion coefficient, density, radius and maximum velocity of the melt; μ_0 is magnetic constant, g is gravitational acceleration.

The characteristic current density j_0 is estimated corresponding to the conductive $j_{0,cond} = I_{el}/(\pi r_{el}^2)$ or to the inductive $j_{0,ind} = I_{ind}/(\delta_{melt} h_{melt}/n)$ power supply with the following parameters: I_{el} is the conductive current over the top electrode with the radius r_{el}; I_{ind} is the effective current in any inductor winding, δ_{melt} is the penetration depth of EM field into the melt, h_{melt} is the height of the melt, n is the number of inductor windings.

The system with nichrome and non-submerged top and bottom DC electrodes (Fig. 2 (a))**.** According to the initial thermal field balance, the heat flux at the arc zone at the melt top surface is q_{spot} *~ 1.29 MW/m^2*. The integral Joule heat in the melt is Q_{melt} *~ 0.017 MW* for a conductive current value I_{el} ~ 100 kA.

The melt flow pattern is characteristic for the EVC due to the conductive DC supply. Maximum velocity is v_{melt} ~ 0.57 m/s. The thermal field is characterized by the expressed temperature gradients near the melt top surface, where the heat flux from the arc is supplied. Since the melt circulation is directed to the center of the arc spot, there is an expressed overheating of the melt with a relatively high value of the difference between the maximum and minimum time-averaged temperature θ ~ 194 K. The TGC is suppressed by the EVC – Al_{cond} ~ 30.7 and Fr_A^{-1} ~ 9.3·10^{-2}.

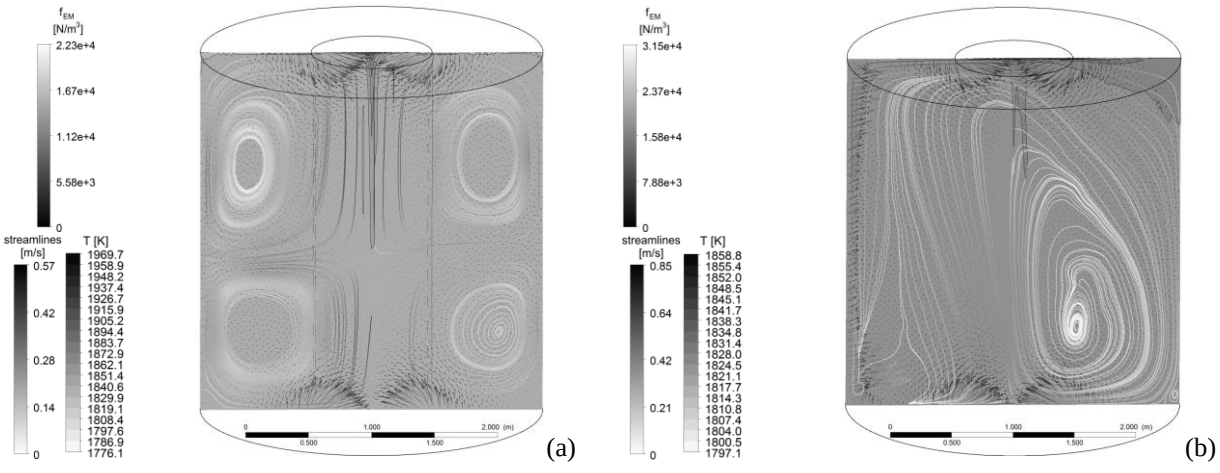

Fig. 2: System with nichrome (σ_{melt} = 6.7·10^5 Ω^{-1}·m^{-1}) and non-submerged top and bottom DC electrodes without (a) and with (b) TMF side inductor: Lorentz force vectors (grayscale) and averaged for flow time t=0–60 s streamlines (inverse grayscale), temperature contours (inverse grayscale)

The system with nichrome and non-submerged top and bottom DC electrodes and TMF side inductor (Fig. 2 (b))**.** According to the initial thermal field balance, the heat flux at the arc zone at the melt top surface is q_{spot} *~ 1.19 MW/m^2*. The integral Joule heat in the melt is Q_{melt} *~ 0.072 MW* for combined power supply – a conductive direct current value

I_{el} ~ 100 kA and a inductive current effective value I_{ind} ~ 50 kA.
The melt circulation is the result of combination of a single vortex of EMC due to the TMF inductor and two toroidal vortices of EVC, when the intensity of EMC is prevailing – Al_{ind} ~ $2.3 \cdot 10^3$ and Al_{cond} ~ 13.2. The totalized circulation consists of a single vortex, which occupies almost whole melt volume. The maximum velocity is v_{melt} ~ 0.85 m/s.
The distribution of thermal field totalize two trends:
• the zone with expressed overheating, which is formed due to the structure of EVC for the zone of spot;
• the drifting of overheating zones due to EMC.
The difference between time-averaged T_{max} and T_{min} is θ ~ 62 K (pronouncedly less than for previous model θ ~ 194 K). The TGC is suppressed (Fr_A^{-1} ~ $1.3 \cdot 10^{-2}$) by both EMC and EVC.

The system with low conductive melt and submerged top and bottom DC electrodes (Fig. 3)**.** According to the initial thermal field balance, the heat fluxes at the surface of electrode tip and at the side surface of electrode are q_{tip}^{el} ~ *0.90 MW/m²* and q_{side}^{el} ~ *0.073 MW/m²*. The integral Joule heat in the melt is Q_{melt} ~ *0.447 MW* for a conductive current value I_{el} ~ 2 kA.
For the development period (t ~ 30 s) (Fig. 3 (a)) the melt flow structure along the side surface of electrode is the result of combination of EVC (clockwise circulation) and TVG (counter clockwise circulation). As the intensity of the melt flow is relatively low with the maximum velocity v_{melt} ~ 0.05 m/s, the overheating temperature θ ~ 451 K.
The developed flow structure of the melt (t ~ 100 s) (Fig. 3 (b)) is characteristic for EVC with two toroidal vortices, maximum velocity v_{melt} ~ 0.13 m/s. Overheating zone of the melt is located near the electrode tip, the difference between the maximum and minimum time-averaged temperature is relatively high with value θ ~ 393 K, which is smaller than in development period. Despite of Froude number for Archimedes force is prevailing – Fr_A^{-1} / Al_{cond} ~ 15.4, the TGC is suppressed due to inconvenience for vortex development in the zone under the tip of electrode with high temperature gradient.

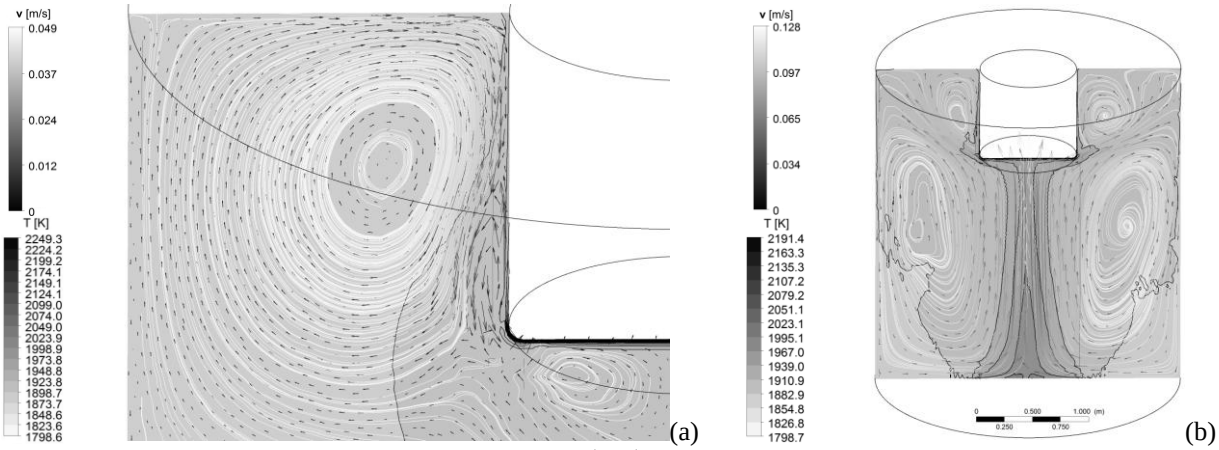

Fig. 3: System with low conductive melt (σ_{melt} = 6.7 $\Omega^{-1} \cdot m^{-1}$) and submerged top and bottom DC electrodes.
Time-averaged streamlines, velocity vectors and temperature contours: flow time (a) t=0–30 s; (b) t = 0–100s.

Conclusions

The overheating zones' locations correspond to the surfaces of (non)submerged electrode, where the heat fluxes are supplied to the melt. The overheating temperature values and the temperature maxima locations depend on the melt flow intensity and pattern.
In the case of high conductive melt the electromagnetic convection is prevailing. The intensity of the thermogravitational convection is comparable with the intensity of the electro-vortex convection only in the case of low conductive melt.

References

[1] S. Pavlovs, A. Jakovics, E. Baake, B. Nacke (2014), Magnetohydrodynamics 50, 303-315
[2] S. Pavlovs, A. Jakovics, V. Sushkovs, B. Nacke (2015), Magnetohydrodynamics 51, 67-81
[3] O. Kazak (2013), Metallurgical and Material Transactions 44B, 1243-1250
[4] S.A. Smirnov, V.V. Kalaev, S.M. Hekhamin, M.M. Krutyanskii, et al. (2010), High Temperature 48, 68-76
[5] G. Djambazov, V. Bojarevics, K. Pericleous (2009), Magnetohydrodynamics 45, 579-586
[6] A. Kharicha, A. Ludwig, M. Wu (2011), 9th Int. Symposium on Liquid Metal Processing and Casting (Nancy, France), 41-48
[7] Z. Wang, N.H. Wang, T. Li (2011), Journal of Materials Processing Technology 211, 388-395